Metallophysics and Advanced Technologies
Металофіз. новітні технол.
Metallofiz. Noveishie Tekhnol.
2025, vol. 47, No. 2, pp. 199–215
https://doi.org/10.15407/mfint.47.02.0199
Reprints available directly from the publisher

PACS numbers: 07.05.Kf, 43.40.Le, 68.35.Iv, 68.60.Bs, 68.65.Ac, 81.15.-z

Investigation of Properties of Multilayer Nitride CrN/NbN Coatings According to Acoustic Emission Parameters. Pt. 1. Multilayer CrN/NbN Coatings with a Double-Layer Thickness of 230 nm

I. V. Serdyuk[*], S. I. Petrushenko[**,***], V. O. Stolbovyy[*,****], and M. Fialkowsky[***]

[*]*National Science Centre*
'Kharkiv Institute of Physics and Technology', N.A.S. of Ukraine,
1 Akademichna Str.,
UA-61108 Kharkiv, Ukraine
[**]*V. N. Karazin Kharkiv National University,*
4 Svobody Sqr.,
UA-61022 Kharkiv, Ukraine
[***]*Technical University of Liberec,*
Studentska 1402/2,
46117 Liberec 1, Czech Republic
[****]*Kharkiv National Automobile and Highway University,*
25 Yaroslava Mudrogo Str.,
UA-61002 Kharkiv, Ukraine

The evaluation method for acoustic emission, which detects the elastic waves emitted during cracking and delamination of the vacuum-arc multilayer nitride CrN/NbN coatings, is used for investigation of the coating properties. The investigation is conducted using scratch testing and microscopic visual observation of scratches. To compare the properties of multilayer CrN/NbN coatings obtained at different technological parameters of deposition as well

Corresponding author: Iryna Vitaliyivna Serdyuk
E-mail: iraserduk@kipt.kharkov.ua

Citation: I. V. Serdyuk, S. I. Petrushenko, V. O. Stolbovyy, and M. Fialkowsky, Investigation of Properties of Multilayer Nitride CrN/NbN Coatings According to Acoustic Emission Parameters. Pt. 1. Multilayer CrN/NbN Coatings with a Double-Layer Thickness of 230 nm, *Metallofiz. Noveishie Tekhnol.*, **47**, No. 2: 199–215 (2025). DOI: 10.15407/mfint.47.02.0199

as to determine and evaluate the processes occurring during the coating deformation, methods for statistical data analysis for acoustic emission are applied. The maximum pulse amplitude, the average value, the median value, the mode value, the number of pulses, and the amplitude sum of all acoustic emission pulses for each coating are calculated. The multilayer CrN/NbN coatings consist of 68 layers with bilayer thickness of 230 nm. To increase the calculation reliability, the studied parameters are calculated on four scratches for each multilayer coating. The influence of deposition technological parameters on the structure deformation processes of multilayer CrN/NbN coatings occurred during scratch testing is determined.

Key words: multilayer coatings, cathodic arc evaporation, acoustic emission, deformation, methods for statistical data analysis, coating embrittlement.

Для дослідження властивостей вакуумно-дугових багатошарових нітридних CrN/NbN покриттів був застосований метод оцінювання акустичної емісії, яка відображає пружні хвилі, що випромінюються під час розтріскування та розшарування цих покриттів. Дослідження проводилися під час скретч-тестування за рахунок оцінювання параметрів акустичної емісії та візуального обстеження подряпин за допомогою мікроскопії. Для порівняння властивостей багатошарових CrN/NbN покриттів, одержаних за різних технологічних параметрів осадження, а також для визначення й оцінювання процесів, що відбуваються за деформації цих покриттів, було застосовано методи статистичної аналізи випадкової величини акустичної емісії. Для кожного багатошарового покриття було визначено максимальну амплітуду імпульсу, середнє значення, медіяну, моду, кількість імпульсів і суму амплітуд усіх імпульсів. Багатошарове CrN/NbN покриття складалося з 68 шарів із двошаровою товщиною у 230 нм. Для підвищення вірогідности розрахунків досліджувані параметри оцінювалися за чотирма подряпинами для кожного багатошарового покриття. Встановлено вплив технологічних параметрів осадження на деформаційні процеси, що відбуваються у структурі багатошарових CrN/NbN-покриттів, під час скретч-тестування.

Ключові слова: багатошарові покриття, вакуумно-дугове осадження, акустична емісія, деформація, методи статистичної аналізи даних, крихкість покриття.

(Received 18 March, 2024; in final version, 8 July, 2024)

1. INTRODUCTION

A variety of methods are used to study the different properties of vacuum arc coatings, which allow to gain new knowledge and expand the application possibilities of these coatings in various fields of science and technology. One of these methods is the measurement of acoustic emission (AE) parameters when studying the physical properties of vacuum arc coatings. This method refers to non-destructive research methods of the solid state. It is based on the registration, processing and analysis of the parameters of mechanical stress waves that occur as a result of the formation, local changes and destruction of the material structure [1–10]. The source of these waves in this acoustic method is the local areas of the studied objects, in which dynamic changes in the structure occur. The change in AE parameters indicates the beginning and dynamics of rapid degradation and relaxation processes in the material structure.

Acoustic emission is a phenomenon of induced spontaneous emission of acoustic waves during the local restructuring of the solid structure, which is accompanied by the formation, disruption, and relaxation of mechanical stresses in local volumes under the action of external fields of various physical natures [9]. Typical AE mechanisms of the solid are the microcracks formation [2, 10], plastic deformation [2, 11–15], phase structural transformations [16], *etc*. In most cases, the AE mechanism, which causes the excitation of acoustic waves, is a certain set of related physical and, additionally, chemical processes occurring in the local volume of material—the source of AE. These processes are accompanied by a short-term release of excess energy, the elastic component of which is the external manifestation of AE [8, 9].

Many investigations have shown that in the process of loading metals or vacuum arc coatings, the AE signal appears only at the beginning of microplastic deformation, that is, it is associated with the movement of crystal lattice defects. Many works [15, 17–37] have been devoted to the study of the acoustic emission nature during deformation processes in metals. The main sources of AE during material deformation are the following dislocation processes [15]: the development of slip lines [27, 29], the propagation of dislocations due to the Frank-Reed source [30, 31], the accelerated movement of dislocations or their movement at high speeds [33, 34], detachment of dislocation loops of critical size from their attachment sites [35, 36], dislocation exit to the free surface and dislocation annihilation [19, 37]. In addition to these, there are other possible sources of AE associated with the presence of impurities and particles of the second phase—cutting of particles by dislocations, decohesion along the interface, *etc*. [15].

Fewer works are devoted to the research of the acoustic emission nature during deformation processes in coatings [38–50]. Determination of AE parameters and the processes that take place when it occurs in vacuum arc multilayer coatings has not yet been widely distributed. The research of these processes in vacuum arc coatings with different architectures will make it possible to control the properties of these coatings by means of changes in their structure. Comparison of AE parameters obtained during deformation processes in vacuum arc coatings of different architecture will allow determining the influence of technological deposition parameters on the structure of vacuum arc multilayer coatings.

This paper presents the research results of AE parameters obtained during loading of multilayer CrN/NbN coatings (bilayer thickness of 230 nm, 68 layers), and the influence of deposition technological parameters on the structure formation processes of these coatings is determined.

2. MATERIALS AND METHODS

2.1. Materials and Deposition

Vacuum arc nitride multilayer CrN/NbN coatings were deposited in a modified installation 'BULAT-6'. The evaporator materials were pure metals of vacuum melting—chromium (Cr99N1) and niobium (Nb1). AISI 430 BA + PVC stainless steel samples with a mirror-polished surface were used as substrates for deposition of coatings. Surface roughness of these samples R_a was lower than 0.05 μm. The dimensions of the samples were 18×18×2 mm. They were used to determine the mechanical and tribological properties of coatings. Before deposition of the vacuum arc coatings, the vacuum chamber with the samples was pumped to a pressure of $P = 1.3 \cdot 10^{-3}$ Pa. After this, the ionic cleaning and activation of the sample surface were carried out by bombardment with metal ions at a constant voltage on its $U_S = -1.1$ kV during ten minutes. After these processes, an underlayer of pure metal was deposited to improve the adhesive properties of the coatings. The technological deposition process of multilayer nitride CrN/NbN coatings to the samples took place within 1.5 hours. The nitrogen pressure in the vacuum chamber P_N varied from 0.08 to 0.27 Pa. The constant negative voltage on the substrate U_S was −70 and −200 V. The arc current of evaporators was 80 A (for chromium) and 100 A (for niobium). The distance from the evaporators to the axis of substrate-holder rotation was 500 mm [51, 52].

2.2. Structural Characterization and Mechanical Testing

Planar raster electron microscopic images were obtained using a Tescan Vega 3 SBU in secondary electron mode at an accelerating voltage of 30 kV. The samples were examined without applying any coatings. The study of physical and mechanical characteristics of coatings on stainless steel samples was carried out by the micro-indentation method using CMS hardness measurement equipped by standard Vickers pyramid. Microhardness numbers were determined under indentation loads not higher than 1.0 N. Microtester capable for load-displacement measurements and equipped by trihedral Berkovich pyramid was used to determine Young's modulus, E, according to the test method procedure originally proposed by Oliver and Pharr. Scratch testing was used for research the tribological properties of multilayer CrN/NbN coatings. It was performed using scratch tester CETR-UMT (Bruker) at linearly increasing load (2–20 N) with velocity of stylus movement 0.1 mm/s during 50.08 s. The time step of measurement is 0.01 s. For these investigations was applied Rockwell diamond indenter (stylus) with 200-μm tip radius. Several parameters of testing were recorded, namely normal and tangential forces, co-ordinates of stylus movement, acoustic emission and friction coefficient. Total scratch length is 5 mm, total scratch depth is in range of 340–360 μm. Four scratches were carried out for each coating to increase accuracy of calculated results.

2.3. Calculations of Research Results

To compare the properties of multilayer CrN/NbN coatings obtained at different deposition technological parameters as well as to evaluate and determine the processes occurring during the coating deformation, methods for statistical data analysis of acoustic emission were applied. The acoustic emission of each coating was evaluated according to the following parameters: the maximum pulse amplitude AE_{max}, the average value AE_{medium}, the median AE_{median}, the mode AE_{moda}, the number of pulses N_{AE} and the amplitudes sum of all acoustic emission pulses SUM_{AE}. The maximum value AE_{max} characterizes the maximum elastic energy released when the coating is deformed. The average value AE_{medium} is the mathematical expectation of a random variable, while the median AE_{median} is the value located in the middle of the ranked AE series. The mode AE_{moda} indicates the value of the random variable that occurs most often in the set of observations. In addition, the scattering characteristics were evaluated for each of the above parameters. To increase the calculations' reliability, the above parameters were evaluated for each multilayer CrN/NbN coating for four scratches.

3. RESULTS AND DISCUSSION

3.1. Parameters of Multilayer Nitride CrN/NbN Coatings and Scratches

Deposition technological parameters of multilayer nitride CrN/NbN coatings (arc current of evaporator (chromium I_{Cr} and niobium I_{Nb}), constant negative voltage on the substrate U_{S}, nitrogen pressure P_{N}) and mechanical properties of these coatings (medium hardness H_{med}, elasticity contact modulus E_{r}, and $H_{\mathrm{med}}/E_{\mathrm{r}}$ ratio) are presented in Table 1 [51].

Table 2 shows the geometric parameters of the multilayer nitride CrN/NbN coatings, namely the thickness of the chromium nitride layer h_{CrN} and niobium nitride layer h_{NbN}, the bilayer period h_{b}, the total coating thickness h, the number of bilayers (periods), and the total

TABLE 1. Technological deposition parameters of multilayer nitride CrN/NbN coatings.

No. sample	Coating composition	I_{Cr}, A	I_{Nb}, A	U_S, V	P_N, Pa	H_{med}, GPa	E_r, GPa	H_{med}/E_r
1	CrN/NbN	80	100	−200	0.27	22.481	317.96	0.056
2	CrN/NbN	80	100	−200	0.08	25.188	312.32	0.064
3	CrN/NbN	80	100	−70	0.27	14.531	250.52	0.05
4	CrN/NbN	80	100	−70	0.08	24.055	279	0.071

TABLE 2. Geometric parameters of multilayer nitride coatings CrN/NbN.

Coating composition	h_{CrN}, nm	h_{NbN}, nm	h_b, nm	h, μm	Number of bilayers	Total number of layers
CrN/NbN	80	150	230	7.8	34	68

number of layers.

Since the total depth of the scratch ($h_{scratch}$ = 340–360 μm) is significantly greater than the total thickness of the multilayer CrN/NbN coating (h = 7.8 μm), then, for a more detailed analysis of the obtained results and separation of the substrate material influence on the calculation results, it is advisable to consider the results obtained at scratch testing in two separate stages, namely,

1) analysis of acoustic emission parameters obtained during time τ upon reaching the equation $h_{scratch} = h = 7.8$ μm,

2) analysis of AE data array obtained during the full test time (T = 50.08 s).

Figure 1 shows photographs of the scratches of the multilayer

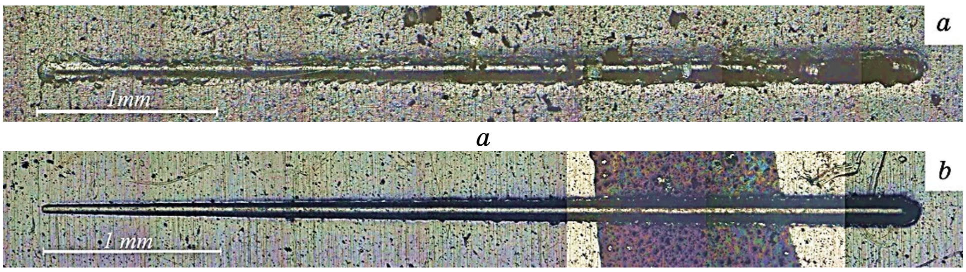

Fig. 1. Scratch of multilayer CrN/NbN coatings (sample No. 1: U_S = −200 V; P_N = 0.27 Pa) (*a*) and scratch of stainless steel sample (substrate) without coating (*b*).

CrN/NbN coating and the uncoated stainless steel test sample (substrate).

3.2. Acoustic Emission Parameters of Multilayer CrN/NbN Coatings. First Research Stage

Table 3 shows the acoustic emission parameters that were obtained during scratch testing of stainless steel sample without coating (for time τ when the equation $h_{scratch} = h = 7.8$ μm is reached), namely the maximum pulse amplitude AE_{max}, the average value AE_{medium}, the median AE_{median}, mode AE_{moda}, number of pulses N_{AE}, root mean square deviation RMSD (N_{AE}) and sum SUM_{AE}.

Table 4 presents the acoustic emission parameters that were obtained during scratch testing of multilayer CrN/NbN coatings when the scratch depth was 7.8 μm. The presented parameters are based on the analysis of 4 scratches for each coating.

Figure 2 shows the dependence of the calculated acoustic emission parameters of multilayer CrN/NbN coatings and the substrate (sample) without coating (line *3*) on constant negative voltage on the substrate (sample) U_S at constant values of the nitrogen pressure P_N in the vacuum chamber (line *1*—$P_N = 0.27$ Pa, line *2*—$P_N = 0.08$ Pa).

Increasing the constant negative voltage on the substrate U_S from −70 to −200 V leads to:

• an increase in the maximum value AE_{max} by 73% at the nitrogen pressure $P_N = 0.27$ Pa and an increase in AE_{max} by 40% at the nitrogen pressure $P_N = 0.08$ Pa, as can be seen in Fig. 2, *a*;

• an increase in the average value AE_{medium} by 66% at the nitrogen

TABLE 3. AE parameters of stainless steel sample without coating.

	AE_{max}, V	AE_{medium}, V	AE_{median}, V	AE_{moda}, V	N_{AE}	RMSD (N_{AE})	SUM_{AE}, V	$h_{scratch}$, μm
Sample	0.18	0.043	0.0417	0.0417	7	10.44	6.38	7.8

TABLE 4. AE parameters of multilayer CrN/NbN coatings.

No. sample	AE_{max}, V	AE_{medium}, V	AE_{median}, V	AE_{moda}, V	N_{AE}	RMSD (N_{AE})	SUM_{AE}, V
1	2.09	0.113	0.0480	0.0459	73.75	78.62	40.31
2	0.42	0.082	0.0627	0.0497	238.67	6.35	29.63
3	1.21	0.068	0.0491	0.0471	90.5	38.65	24.81
4	0.30	0.060	0.0521	0.0479	152.67	49.52	21.14

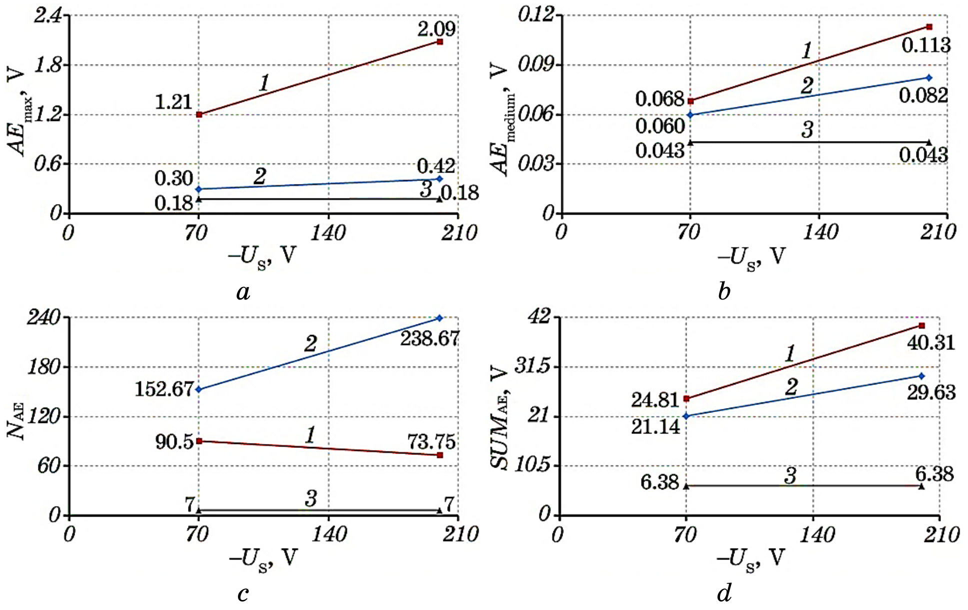

Fig. 2. Dependence graphs of acoustic emission parameters of multilayer CrN/NbN coatings and substrate on the deposition technological parameter U_S at constant values of the nitrogen pressure in the vacuum chamber P_N: AE_{max} (*a*), AE_{medium} (*b*), N_{AE} (*c*), SUM_{AE} (*d*).

pressure $P_N = 0.27$ Pa and an increase in AE_{medium} by 37% at the nitrogen pressure $P_N = 0.08$ Pa, as can be seen in Fig. 2, *b*;

• a decrease in the median value AE_{median} from 0.0491 V to 0.0480 V at the nitrogen pressure $P_N = 0.27$ Pa (by 2%, which is within calculation error) and an increase in AE_{median} by 20% (from 0.0521 V to 0.0627 V) at the nitrogen pressure $P_N = 0.08$ Pa, as can be seen in Table 4;

• changes in the mode value AE_{moda} are within 2.5% and 3.75% at the nitrogen pressure $P_N = 0.27$ Pa and 0.08 Pa, respectively, as can be seen in Table 4;

• a decrease in the value N_{AE} by 18.5% at the nitrogen pressure $P_N = 0.27$ Pa, as can be seen in Fig. 2, *c*. At the same time root mean square deviation RMSD (N_{AE}) increases by 2 times (from 38.65 to 78.62), as can be seen in Table 4;

• an increase in the value N_{AE} by 56% at the nitrogen pressure $P_N = 0.08$ Pa, as can be seen in Fig. 2, *c*, and root mean square deviation RMSD (N_{AE}) decreases by 7.8 times (from 49.52 to 6.35), as can be seen in Table 4;

• an increase in the value SUM_{AE} by 62.5% at the nitrogen pressure $P_N = 0.27$ Pa and an increase in SUM_{AE} by 40% at the nitrogen pressure $P_N = 0.08$ Pa, as can be seen in Fig. 2, *d*.

Figure 3 shows the dependence of the calculated acoustic emission parameters of multilayer CrN/NbN coatings and the substrate (line *3*) on the nitrogen pressure P_N at constant negative voltage on the substrate U_S (line *1*—$U_S = -70$ V, line *2*—$U_S = -200$ V).

Increasing in the nitrogen pressure P_N in the vacuum chamber from 0.08 to 0.27 Pa leads to:

• an increase in the maximum value AE_{max} by 4 and 5 times at the constant negative voltage on the substrate $U_S = -70$ V and -200 V, respectively, as can be seen in Fig. 3, *a*;

• an increase in the average value AE_{medium} by 13% and 38% at the constant negative voltage on the substrate $U_S = -70$ V and -200 V, respectively, as can be seen in Fig. 3, *b*;

• a decrease in the median value AE_{median} by 6% (from 0.0521 V to 0.0491 V) and 23.5% (from 0.0627 V to 0.0480 V) at the constant negative voltage on the substrate $U_S = -70$ V and -200 V, respectively, as can be seen in Table 4;

• a decrease in the mode value AE_{moda} by 1.7% and 7.7% at the constant negative voltage on the substrate $U_S = -70$ V and -200 V, respectively, as can be seen in Table 4;

• a decrease in the value N_{AE} by 1.7 and 3.3 times at the constant

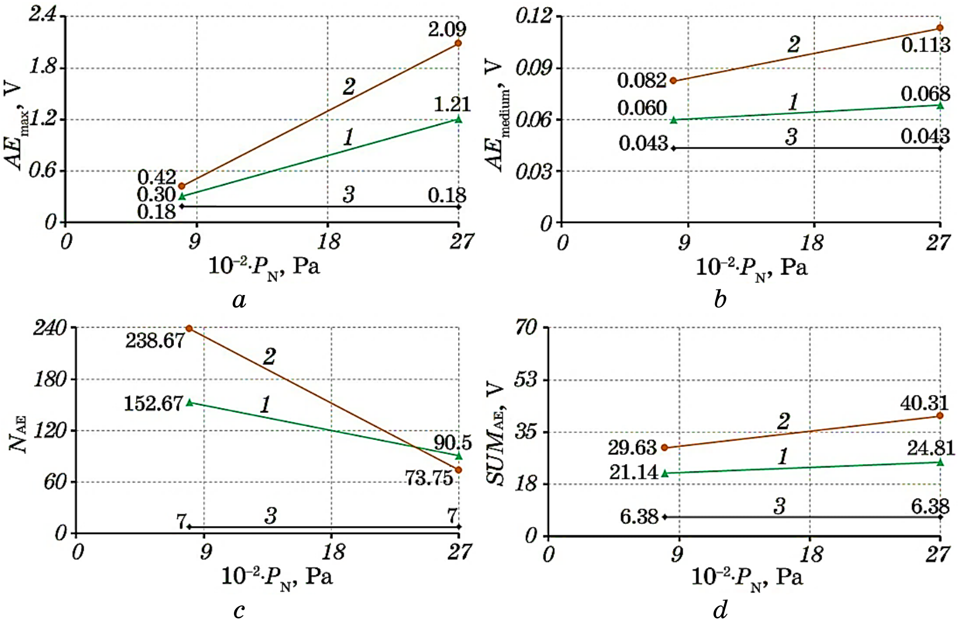

Fig. 3. Dependence graphs of acoustic emission parameters of multilayer CrN/NbN coatings and substrate on the deposition technological parameter P_N at the constant negative voltage on the substrate U_S: AE_{max} (*a*), AE_{medium} (*b*), N_{AE} (*c*), SUM_{AE} (*d*).

negative voltage on the substrate $U_S = -70$ V and -200 V, respectively, as can be seen in Fig. 3, *c*;

• an increase in the value SUM_{AE} by 17.4% and 36% at the constant negative voltage on the substrate $U_S = -70$ V and -200 V, respectively, as can be seen in Fig. 3, *d*.

The graphs in Figures 2, 3 clearly demonstrate the local structure reconstruction of the multilayer CrN/NbN coating, which is accompanied by the formation, breakdown and relaxation of mechanical stresses in local volumes of the coating under the load action ($F = 2.8$ H).

The analysis of the research results showed that constant negative voltage on the substrate U_S has the greatest effect on the average value AE_{medium} and the sum SUM_{AE}, while the nitrogen pressure P_N in the vacuum chamber affects the maximum values AE_{max} and the amount N_{AE}.

The increase of all AE parameters with increasing voltage U_S at nitrogen pressure $P_N = 0.08$ Pa is characteristic at this research stage, while increasing voltage U_S at the pressure $P_N = 0.27$ Pa leads to a decrease in the parameter N_{AE}, but total SUM_{AE} increases due to an increase in the maximum value AE_{max}.

The trend of changes in AE parameters with increasing pressure P_N is preserved both at voltage $U_S = -70$ V and at $U_S = -200$ V, *i.e.*, the parameters AE_{max}, AE_{medium} increase, but AE_{median}, AE_{moda}, N_{AE} and SUM_{AE} decrease. The analysis of the parameter RMSD (N_{AE}) showed that an increase in voltage U_S at the pressure $P_N = 0.08$ Pa leads to a significant decrease (by 7.8 times) in RMSD (N_{AE}), and an increase in voltage U_S at the pressure $P_N = 0.27$ Pa leads to a 2-fold increase in RMSD (N_{AE}). These results show structural heterogeneity within the volume of the entire CrN/NbN coating and indicate the presence of local microvolumes in the coating with a greater number of defects (dislocations, vacancies, *etc.*). The multilayer coating structure CrN/NbN (68 layers with layer thicknesses $h_{CrN} = 80$ nm, $h_{NbN} = 150$ nm) also affects the studied parameters.

3.3. Acoustic Emission Parameters of Multilayer CrN/NbN Coatings. Second Research Stage

Table 5 shows the acoustic emission parameters that were obtained during scratch testing of the uncoated stainless steel sample over the full research time ($T = 50.08$ s), namely, the maximum pulse amplitude AE_{max}, the average value AE_{medium}, the median AE_{median}, the mode AE_{moda}, number of pulses N_{AE}, root mean square deviation RMSD (N_{AE}), sum of amplitudes of all acoustic emission pulses SUM_{AE}, and scratch depth $h_{scratch}$.

Table 6 presents the acoustic emission parameters that were obtained during scratch testing of multilayer CrN/NbN coatings for the full time of research ($T = 50.08$ s). The presented parameters are based on the analysis of 4 scratches for each coating.

TABLE 5. AE parameters of stainless steel sample without coating.

	AE_{max}, V	AE_{medium}, V	AE_{median}, V	AE_{moda}, V	N_{AE}	RMSD (NAE)	SUM_{AE}, V	$h_{scratch}$, μm
Sample	8.5	0.252	0.0615	0.0414	1079	88.3	506	347.3

TABLE 6. AE parameters of multilayer CrN/NbN coatings.

No. sample	AE_{max}, V	AE_{medium}, V	AE_{median}, V	AE_{moda}, V	N_{AE}	RMSD (N_{AE})	SUM_{AE}, V	$h_{scratch}$, μm
1	3.06	0.159	0.0550	0.0471	2592	166	794	348.8
2	2.64	0.175	0.1298	0.0675	4802	65	876	348.6
3	6.80	0.230	0.0599	0.0481	2961	518	1152	355.3
4	3.26	0.105	0.0782	0.0579	4259	115	527	343.1

Figure 4 shows the dependences of the calculated acoustic emission parameters of multilayer CrN/NbN coatings and the substrate (sample) without coating (line *3*) on the constant negative voltage on the substrate (sample) U_S at constant values of the nitrogen pressure P_N in the vacuum chamber (line *1*—$P_N = 0.27$ Pa, line *2*—$P_N = 0.08$ Pa).

Increasing the constant negative voltage on the substrate U_S from −70 to −200 V leads to:

• a decrease in the maximum value AE_{max} by 20% and 55% at the nitrogen pressure $P_N = 0.08$ Pa and 0.27 Pa, respectively, as can be seen in Fig. 4, *a*;

• an increase in the average value AE_{medium} by 66.7% at the nitrogen pressure $P_N = 0.08$ Pa and a decrease in AE_{medium} by 31% at the nitrogen pressure $P_N = 0.27$ Pa, as can be seen in Fig. 4, *b*;

• an increase in the median value AE_{median} by 66% at the nitrogen pressure $P_N = 0.08$ Pa and a decrease in AE_{median} by 8.3% at the nitrogen pressure $P_N = 0.27$ Pa, as can be seen in Table 6;

• an increase in the mode value AE_{moda} by 16.6% at the nitrogen pressure $P_N = 0.08$ Pa and a decrease in AE_{moda} by 2% at the nitrogen pressure $P_N = 0.27$ Pa, as can be seen in Table 6;

• an increase in the value N_{AE} by 12.7% at the nitrogen pressure $P_N = 0.08$ Pa and a decrease in N_{AE} by 12.5% at the nitrogen pressure $P_N = 0.27$ Pa, as can be seen in Fig. 4, *c*;

• a decrease in the value RMSD (N_{AE}) by 43.5% and 68% at the nitrogen pressure $P_N = 0.08$ Pa and 0.27 Pa, respectively, as can be seen in Table 6;

• an increase in the value SUM_{AE} by 66% at the nitrogen pressure $P_N = 0.08$ Pa and a decrease in SUM_{AE} by 31% at the nitrogen pressure $P_N = 0.27$ Pa, as can be seen in Fig. 4, *d*.

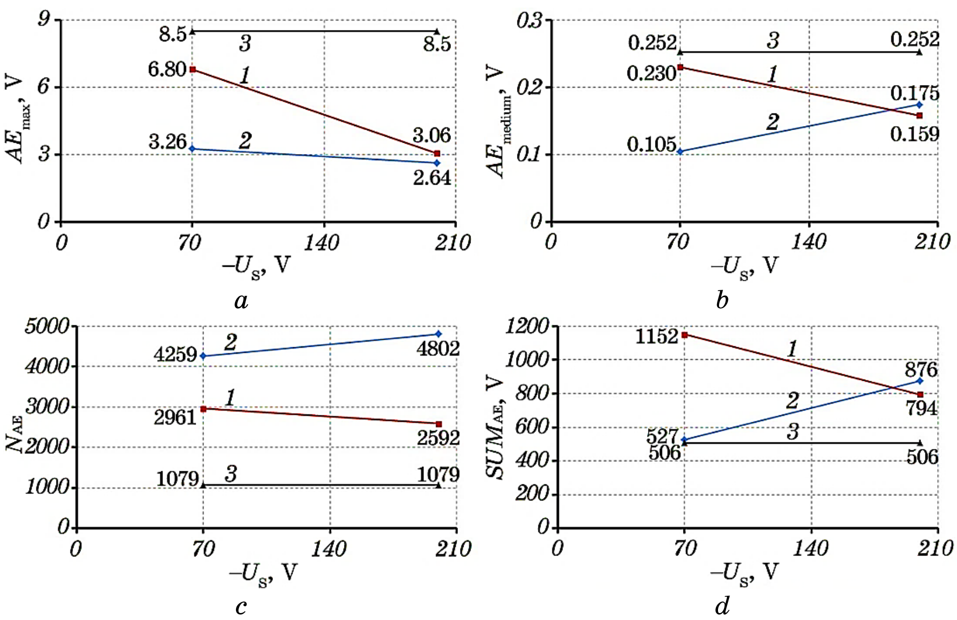

Fig. 4. Dependence graphs of acoustic emission parameters of multilayer CrN/NbN coatings and the substrate on the deposition technological parameter U_S at constant values of the nitrogen pressure in the vacuum chamber P_N: AE_{max} (*a*), AE_{medium} (*b*), N_{AE} (*c*), SUM_{AE} (*d*).

Figure 5 shows the dependence of the calculated acoustic emission parameters of multilayer CrN/NbN coatings and the substrate (line *3*) on the nitrogen pressure P_N at the constant negative voltage on the substrate U_S (line *1*—$U_S = -70$ V, line *2*—$U_S = -200$ V).

Increasing in the nitrogen pressure P_N in the vacuum chamber from 0.08 to 0.27 Pa leads to:

• an increase in the maximum value AE_{max} by 108.6% and 16% at the constant negative voltage on the substrate $U_S = -70$ V and −200 V, respectively, as can be seen in Fig. 5, *a*;

• an increase in the average value AE_{medium} by 119% at the constant negative voltage on the substrate $U_S = -70$ V and a decrease in AE_{medium} by 9% at the constant negative voltage on the substrate $U_S = -200$ V, as can be seen in Fig. 5, *b*;

• a decrease in the median value AE_{median} by 23.3% and 57.6% at the constant negative voltage on the substrate $U_S = -70$ V and −200 V, respectively, as can be seen in Table 6;

• a decrease in the mode value AE_{moda} by 17% and 30% at the constant negative voltage on the substrate $U_S = -70$ V and −200 V, respectively, as can be seen in Table 6;

• a decrease in the value N_{AE} by 30.5% and 46% at the constant nega-

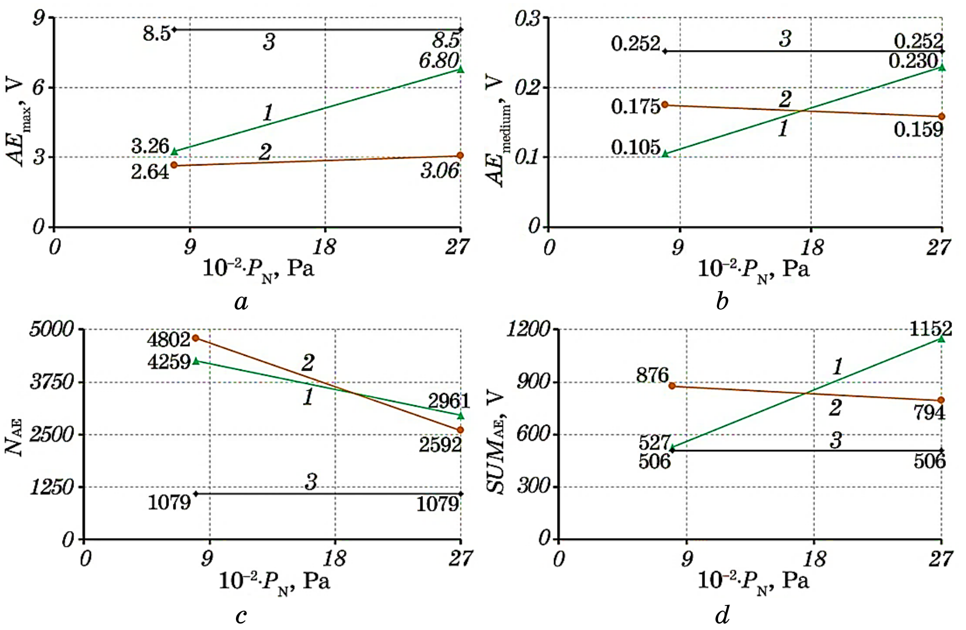

Fig. 5. Dependence graphs of acoustic emission parameters of multilayer CrN/NbN coatings and the substrate on the deposition technological parameter P_N at the constant negative voltage on the substrate U_S: AE_{max} (*a*), AE_{medium} (*b*), N_{AE} (*c*), SUM_{AE} (*d*).

tive voltage on the substrate $U_S = -70$ V and -200 V, respectively, as can be seen in Fig. 5, *c*;

• an increase in the value RMSD (N_{AE}) by 4.5 and 2.5 times at the constant negative voltage on the substrate $U_S = -70$ V and -200 V, respectively, as can be seen in Table 6;

• an increase in the value SUM_{AE} by 118.6% at the constant negative voltage on the substrate $U_S = -70$ V and a decrease in SUM_{AE} by 9.4% at the constant negative voltage on the substrate $U_S = -200$ V, as can be seen in Fig. 5, *d*.

The graphs in Figures 4, 5 clearly demonstrate the local structure reconstruction of the multilayer CrN/NbN coating together with the substrate, which is accompanied by the formation, breakdown and relaxation of mechanical stresses in local volumes of not only the coating, but also the substrate under the action of a higher load ($F = 20$ N).

The analysis of AE parameters at this research stage showed that the nitrogen pressure P_N affects the parameter N_{AE} the most. The increase in P_N leads to a decrease in N_{AE}. It can be related to the number of nitrogen atoms in the coating and its stoichiometry.

AE parameter comparison between the coating and the uncoated substrate showed that the multilayer CrN/NbN coating reduced the parameter AE_{max} and AE_{medium}. The higher values of the parameters N_{AE} and SUM_{AE} of the coated substrate indicate a significant contribution of the coating (even when the scratch depth is greater than the coating thickness).

Figure 6 shows the scratch and the acoustic emission amplitude AE observed when a substrate with the multilayer CrN/NbN coating (technological parameters of deposition $U_S = -200$ V and $P_N = 0.27$ Pa) is scratched.

The amplitude and shape of the AE peaks are affected not only by the physical and chemical properties of the coating components (CrN and NbN), but also by the architecture of the multilayer coating, namely, the number of layers and their thicknesses, properties of the interlayer boundary, *etc*.

4. CONCLUSION

The dependence of the acoustic emission parameters on the deposition technological parameters (constant negative voltage on the substrate U_S, nitrogen pressure P_N) was investigated. This study characterizes the multilayer CrN/NbN coating with 68 layers (34 bilayers), bilayer thickness $h_b = 230$ nm.

The obtained research results can be summarized in the form of the following conclusions.

An increase in the technological parameters (U_S, P_N) leads to an increase in the parameter AE_{max} during total time of the study ($T = 50.08$ s). At the same time, the growth of AE_{max} is more significant at the beginning of the scratch.

An increase in the technological parameter U_S leads to an increase in the parameter AE_{medium} at the beginning of the scratch, but at the same time AE_{medium} decreases along the entire length of the scratch.

The change trend of the parameter AE_{median}, which characterizes the median value by position, remains unchanged both at the beginning of the scratch and along its entire length, depending on the technological parameter (U_S, P_N) of the coating deposition. The change range of the parameter AE_{median} is from 2% to 23.5% at the beginning of the scratch and from 8.3% to 66% along the entire length of the scratch.

The change trend of the parameter N_{AE} depending on the technological parameter of coating deposition remains unchanged along the entire length of the scratch. The change range of the parameter N_{AE} is from 18.5% to 70% at the beginning of the scratch and from 12.5% to 46% along the entire length of the scratch.

At the beginning of the scratch, the parameter SUM_{AE} increases with the growth of all technological parameters of coating deposition, but along the entire length of the scratch, it changes this trend.

The above observations make it possible to study the changes in the

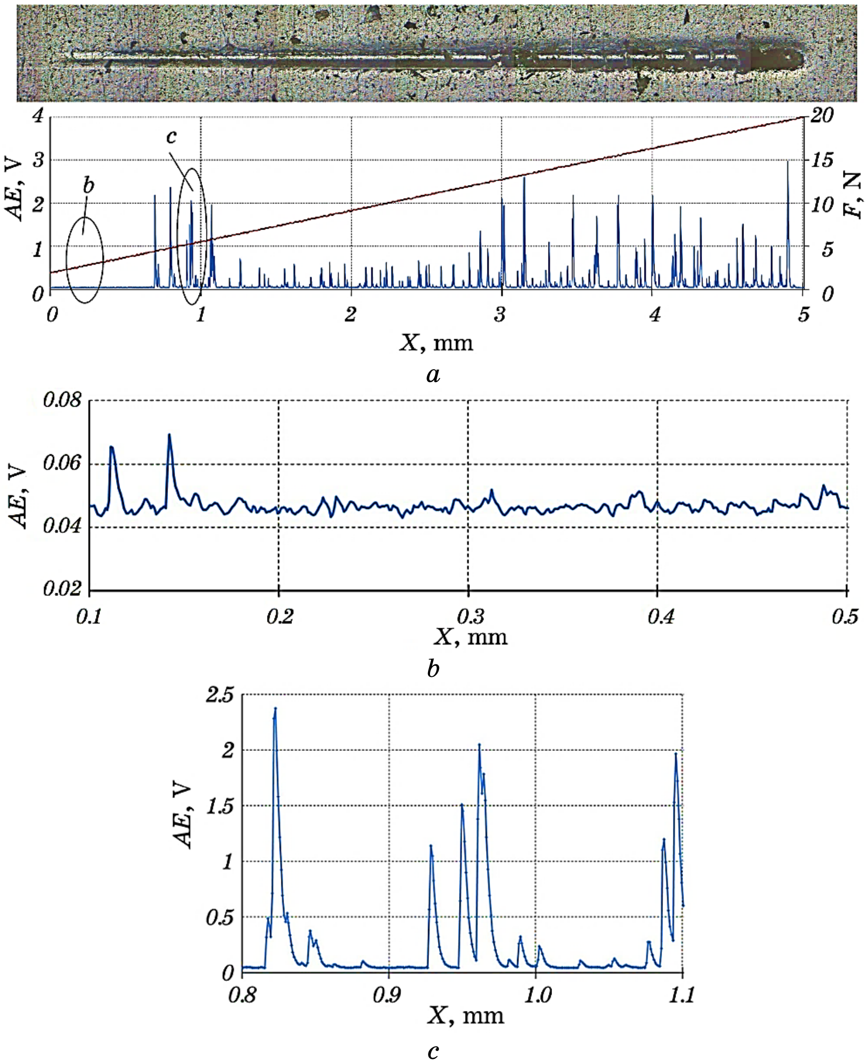

Fig. 6. Scratch and acoustic emission *AE* of the multilayer CrN/NbN coating ($U_S = -200$ V, $P_N = 0.27$ Pa). Dependence of the acoustic emission *AE* on the movement of diamond indenter (stylus): scratch length $X = 5$ mm (*a*), scratch length *X* from 0.1 to 0.5 mm (*b*), scratch length *X* from 0.8 to 1.1 mm (*c*).

coating structure under loading along the entire scratch length and to predict the structural properties of the coatings depending on the deposition technological parameters and the coating architecture.

The obtained research results will be used in the future to compare the behaviour of multilayer CrN/NbN coatings with different architectures, namely with reduced bilayer thickness and increased number of layers, under load (scratch testing). This will make it possible to expand the data array and simplify further prediction of the properties of multilayer coatings.

REFERENCES

1. V. M. Perga, *Novi Metody Doslidzhennya Fizychnykh Vlastyvostei Tverdykh Til. Akustychna Emisiya. Chastyny 1 i 2* [New Methods of Studying the Physical Properties of Solid Bodies. Acoustic Emission. Parts 1 and 2] (Kyiv: 1991).
2. O. V. Gusev, *Akustycheskaya Emissiya pri Deformatsii Monokristallov Tugoplavkikh Metallov* [Acoustic Emission During Deformation of Single Crystals of Refractory Metals] (Moskva: Nauka: 1982).
3. V. A. Kalitenko, V. M. Perga, and I. N. Salivonov, *Phys. Solid State*, **22**, No. 6: 1838 (1980).
4. O. V. Lyashenko and V. P. Veleshchuk, *Ukr. J. Phys.*, **48**, No. 9: 981 (2003) (in Ukrainian).
5. M. V. Kravtsov, O. V. Lyashenko, and A. P. Onanko, *Funct. Mater.*, **11**, No. 2: 353 (2004).
6. V. I. Artyukhov, K. B. Vakar, and V. I. Makarov, *Akusticheskaya Emissiya i Yeyo Primenenie dlya Nerazrushayushchego Kontrolya v Yadernoi Ehnergetike* [Acoustic Emission and its Application for Non-Destructive Testing in Nuclear] (Moskva: Atomizdat: 1980).
7. A. E. Lord and W. Mason, *Phys. Acoustic*, **11**: 289 (1975).
8. *DSTU 2374-94, Rozrakhunky na Mitsnist ta Vyprobuvannya Tekhnichnykh Vyrobiv. Akustychna Emisiya* [Strength Calculations and Testing of Technical Products Acoustic Emission] (Kyiv: Derzhstandart Ukrainy: 1994) (in Ukrainian).
9. O. I. Vlasenko, M. P. Kyseliuk, V. P. Veleshchuk, Z. K. Vlasenko, I. O. Lyashenko, and O. V. Lyashenko, *Optoelectronics and Semiconductor Technique*, **49**: 5 (2014) (in Ukrainian).
10. V. P. Babak and S. F. Filonenko, *Advances in Aerospace Technology*, **1**, No. 1: 54 (1998) (in Ukrainian).
11. G. I. Prokopenko, T. V. Golub, O. N. Kashevskaya, B. N. Mordyuk, N. A. Efimov, and V. G. Bezkorovainyi, *Metallofiz. Noveishie Tekhnol.*, **28**, No. 2: 151 (2006).
12. P. I. Stoev, I. I. Papirov, and V. I. Moschenok, *Probl. Atom. Sci. Tech.*, **1**: 15 (2006).
13. A. M. Leskovskyi and Sh. Sh. Azimov, *Tech. Phys. Lett.*, **10**, No. 5: 307 (1997).
14. L. V. Tikhonov and G. I. Prokopenko, *Tech. Diagnostics and Non-Dictructive Testing*, **8**: 73 (1991).
15. A. Yu. Vinogradov and D. L. Merson, *Low Temp. Phys.*, **44**, No. 9: 1186 (2018).
16. V. A. Kalitenko, I. Ya. Kucherov, V. M. Perga, and V. A. Tkhoryk, *Phys. Solid State*, **30**, No. 12: 3677 (1988).
17. A. M. Kosevich and V. S. Boyko, *Physics-Uspekhi*, **104**: 201 (1971).
18. J. D. Eshelby, *Proc. Roy. Soc.*, **260**: 222 (1962).
19. N. Kiesewetter and P. Schiller, *Scr. Met.*, **8**: 249 (1974).
20. B. Polyzos, E. Douka, and A. Trochidis, *J. Appl. Phys.*, **89**: 2124 (2001).
21. D. G. Eitzen and H. N. G. Wadley, *J. Res. Natl. Bur. Stand.*, **89**: 75 (1984).

22. A. Trochidis and B. Polyzos, *J. Appl. Phys.*, **78**: 170 (1995).
23. A. M. Kosevich, *Zh. Eksp. Teor. Fiz*, **42**: 152 (1962).
24. A. M. Kosevich, *Ukr. J. Phys.*, **84**: 579 (1964).
25. A. Trochidis and B. Polyzos, *J. Mech. Phys. Solids*, **42**: 1933 (1994).
26. A. Sendrowicz, A. O. Myhre, A. V. Danyuk, and A. Vinogradov, *Mater. Sci. Eng. A*, **856**: 143969 (2022).
27. Yu. B. Drobot and V. V. Korchevsky, *Flaw Detection*, **6**: 38 (1985).
28. V. R. Skalskyi, Yu. Ya. Matviiv, and O. G. Simakovych, *Physicochemical Mechanicals of Materials*, **48**, No. 6: 76 (2012).
29. R. M. Fisher and L. S. Lally, *Canad. J. Phys.*, **45**: 1147 (1967).
30. T. Imanaka and K. Sano, *Crystal Lattice Def.*, **4**: 57 (1973).
31. J. R. Frederick and D. K. Felbeck, *Acoustic Emission* (Baltimore: ASTM STP: 1972).
32. N. H. Faisal, R. Ahmed, and R. L. Reuben, *Int. Mat. Rev.*, **56**, No. 2: 98 (2011).
33. D. Rouby and P. Fleischmann, *Internal Friction and Ultrasonic Attenuation Solids* (1977), p. 811.
34. C. B. Scruby and H. N. G. Wadley, *Met. Science*, **15**: 599 (1981).
35. F. P. Higgins and S. N. Carpenter, *Acta Metallurg.*, **26**: 133 (1978).
36. D. R. James and S. N. Carpenter, *J. Appl. Phys.*, **42**: 4685 (1971).
37. V. S. Boyko, V. F. Kivshik, and L. F. Krivenko, *Zh. Eksp. Teor. Fiz*, **78**: 797 (1980).
38. J. Tomastik, R. Ctvrtlik, P. Bohac, M. Drab, V. Koula, K. Cvrk, and L. Jastrabik, *Key Eng. Mater.*, **662**: 119 (2015).
39. J. Tomastik, R. Ctvrtlik, M. Drab, and J. Manak, *Coatings*, **8**, No. 5: 196 (2018).
40. S. Yamamoto and H. Ichimura, *J. Mater. Res.*, **7**: 2240 (1992).
41. Nicholas X. Randall, *Surf. Coat. Tech.*, **380**: 125092 (2019).
42. H. Jensen, U. M. Jensen, and G. Sorensen, *Surf. Coat. Technol.*, **74–75**: 297 (1995).
43. R. K. Choudhary and P. Mishra, *J. Mater. Eng. Perform.*, **25**: 2454 (2016).
44. Tian-Shun Dong, Ran Wang, Guo-Lu Li, and Liu Ming, *High Temp. Mater. Proc.*, **38**: 601 (2019).
45. P. Drobny, D. Mercier, V. Koula, S. I. Škrobáková, L. Čaplovič, and M. Sahul, *Coatings*, **11**, No. 8: 919 (2021).
46. M. A. Hassan, A. R. Bushroa, and R. Mahmoodian, *Surf. Coat. Tech.*, **277**: 216 (2015).
47. B. Warcholiński, A. Gilewicz, Z. Kukliński, and P. Myśliński, *Vacuum*, **83**, No. 4: 715 (2008).
48. E. Hamzah, M. Ali, and M. R. HJ. Mohd Toff, *Surf. Rev. Lett.*, **13**, No. 6: 763 (2006).
49. T. Z. Kattamis, F. Chang, and M. Levy, *Surf. Coat. Tech.*, **43–44**, No. 1: 390 (1990).
50. K. Ikenaga, A. Yanagida, and A. Azushima, *Journal of Solid Mechanics and Materials Engineering*, **3**, No. 2: 347 (2009).
51. I. V. Serdiuk, S. I. Petrushenko, V. O. Stolbovyi, and M. Fijalkowski, *Metallofiz. Noveishie Tekhnol.*, **46**, No. 1: 23 (2024).
52. V. P. Rudenko, V. O. Stolbovoy, I. V. Serdiuk, and K. G. Kartmazov, *East.-Eur. J. Enterp. Tech.*, **48**, No. 6/1: 66 (2010).